

## The Airborne Seeker Test Bed

The Airborne Seeker Test Bed is a recently operational instrumentation system containing a closed-loop tracking, semi-active seeker with the capability to record high-fidelity signals pertaining to radar seeker phenomenology, target scattering characteristics, electronic countermeasures, and acquisition and tracking performance. The unique capabilities of the test bed will be used to collect data and develop computer models for evaluating and predicting missile performance. Test bed data will be used to evaluate the susceptibility of U.S. aircraft to missile attack, and to explore new directions for future systems. The test bed is also designed to support the development of advanced seekers and new electronic counter-countermeasure techniques, and to demonstrate their capabilities in flight.

Major problems in missile seeker design are target-detection sensitivity and the effects of ground clutter and modern electronic countermeasures (ECM). The low radar cross section of weapons such as cruise missiles and future fighter and bomber aircraft, as well as the ability of modern targets to fly at low altitudes, makes the missile intercept problems even more difficult. In addition, the effectiveness of certain modern countermeasures at degrading missile performance is not well understood. These problems combine to present stressing challenges to current missile defenses.

Lincoln Laboratory has undertaken a significant effort to help solve these seeker problems, with the initial emphasis on radar-guided missiles. The central element in this effort is the Airborne Seeker Test Bed, a flying instrumentation system that carries a closed-loop tracking seeker and also records high-fidelity signals related to radar phenomenology (clutter, multipath), target scattering characteristics (bistatic radar cross section, scintillation statistics, angle glint), ECM, and overall seeker acquisition and tracking performance. The purpose behind the development of these capabilities is to collect data and to develop computer models that will assist in the design of future seekers and in the prediction of missile performance. Measured data from the test bed will be used to evaluate the susceptibility of U.S. aircraft to missile attack and to investigate new concepts for future

systems. Specific features have been designed and incorporated into the test bed to support the development of techniques for electronic counter-countermeasures (ECCM), and to demonstrate those techniques in flight.

The *seeker* is the system on the missile that performs the on-board target sensing for flight guidance, with the ultimate purpose of bringing the intercepting missile's warhead within a lethal radius of the target. Because of advances in radar cross-section reduction techniques and ECM, future seekers will face increasingly sophisticated threats. In fact, the advent of low radar cross-section air vehicles has made countermeasures more attractive because the radiated power necessary to mask a vehicle's radar return has decreased to the point where small countermeasure devices are now practical.

Future radar seekers will require higher sensitivity and more effective clutter rejection. These seekers will probably incorporate dual polarization sensors and multispectral sensors, such as a combination of infrared and radar. The future enhancements will help discriminate and reject false targets, including decoys. As a consequence, the burden of decision making on board the seeker will increase, as will the associated complexity in signal processing. The system architecture of the Airborne Seeker Test Bed was selected to address this set of seeker problems.

## Seeker Performance Issues

The ability of a missile to intercept a target is often limited by seeker sensitivity, ground-clutter rejection, or ECM immunity. The specific waveform used by the seeker, which provides varying degrees of resolution in Doppler frequency and range, also has performance implications. These subjects are reviewed in the following paragraphs.

### *Seeker Sensitivity*

Low cross-section targets tax the capabilities of intercepting missiles by requiring them to be more sensitive to target detection in the presence of natural thermal noise. The following methods can increase the sensitivity of a missile system:

1. *Increase transmitter power.* For example, doubling the transmitter power would increase the free-space detection range by a factor of 1.2 on a given target.
2. *Increase transmitter and/or receiver antenna gains.* Doubling the dimensions of one of the antennas would increase the free-space detection range by a factor of 1.4 on a given target. In practice, the narrow diameter of a missile restricts antenna size, which also restricts achievable antenna gain. Typical air-to-air missile seeker antennas are 5 to 7 in in diameter; similar antennas for surface-to-air missiles range from 9 to 16 in.
3. *Lower the receiver noise floor.* Current systems have noise floors within 4 to 10 dB of theoretical limits. A 3-dB improvement (which is a challenge to achieve) would increase the free-space detection range by a factor of 1.2 on a given target.
4. *Increase the received signal integration period.* A longer signal integration period would reduce the effect of thermal noise. Faster signal processing could lead to integration periods up to 10 times longer than current systems, an increase in integration that could extend the free-space detection range by a factor of 1.8. The benefits of integration are limited, how-

ever, because the accelerations of target maneuvering smear the signal and make the integration ineffective beyond a certain period.

Significant performance gains are difficult to achieve, as indicated in the first three categories listed above. Even the gains created by a longer signal integration period could be insufficient for future low cross-section targets. A possible solution to the sensitivity problem is to launch the missile and guide it remotely by a powerful command-guidance system out to a range close enough for the seeker to detect the target. The command-guidance radar would be a larger system that could solve the sensitivity problem by increasing transmitter power and/or antenna gain. The seeker in these systems would need the capability to acquire the target autonomously, since the command guidance may be unable to put the seeker onto the target directly. Whatever missile system architecture is considered, the seeker performance implications of the low cross-section threat, and concepts for possible improvements, provide a significant challenge.

### *Ground Clutter*

Even if the seeker possesses enough sensitivity, the ground clutter can limit performance by masking the target return. Figure 1 illustrates the clutter environment as viewed by the missile. The specific case shown is for a semi-active surface-to-air missile with continuous-wave (CW) illumination (see the box titled "Radar-Guided Missiles" for a definition of missile types). For outbound targets (the *tail chase* scenario), ground clutter seen through the antenna sidelobes directly obscures the target return. For inbound targets, the target return competes with the noise sidebands from the missile's receiver oscillators (and other system-specific sources), which spill into what would have been a clutter-free portion of the Doppler spectrum. The level of these noise sidebands is proportional to the strongest signal (usually main-beam clutter) in the receiver. If the target is high enough in Doppler frequency (which corresponds to a high missile-to-target closing ve-

locity), the target will appear in a region of the spectrum where the noise sidebands have reached a floor level. In low-clutter situations this floor level is the thermal noise floor of the receiver.

Figure 1 indicates that the missile is more capable of intercepting targets in the incoming target region than in the outgoing target region. Therefore, air vehicle designers must generally emphasize lowering the nose cross section to enhance a vehicle's ability to penetrate radar defenses.

Signal integration reduces the effective level of the noise sidebands, with respect to the target signal, and reduces the sidelobe clutter. The seeker designer further combats the effects of clutter by attempting to achieve low sidelobes on the antenna and high oscillator stability (low-noise sidebands) in the receiver.

### Electronic Countermeasures

Many categories of ECM currently exist. Certain ECM techniques are designed to exploit

an idiosyncratic Achilles' heel in the threat system. For example, a missile that relies on three consecutive signal bursts to perform target-angle measurement can be confused by a distorted or amplified signal sent by the target every third burst. The idiosyncratic techniques generally exploit some vulnerable characteristic of the victim's receiver architecture, signal processing technique, or control logic (and consequently require a knowledge of the characteristic). These ECM techniques are generally classified, since the enemy can eliminate the specific vulnerability if the weakness being exploited is known.

Other more fundamental techniques are difficult to overcome, even if the enemy has knowledge of them. A decoy deployed by the target, for example, can be an actual radar target, physically separated from the true target. Since the decoy is a real target, the seeker cannot eliminate it by a simple change in processing algorithm. We must devise a more complicated method to discriminate the true target from the decoy. In addition to expendable or

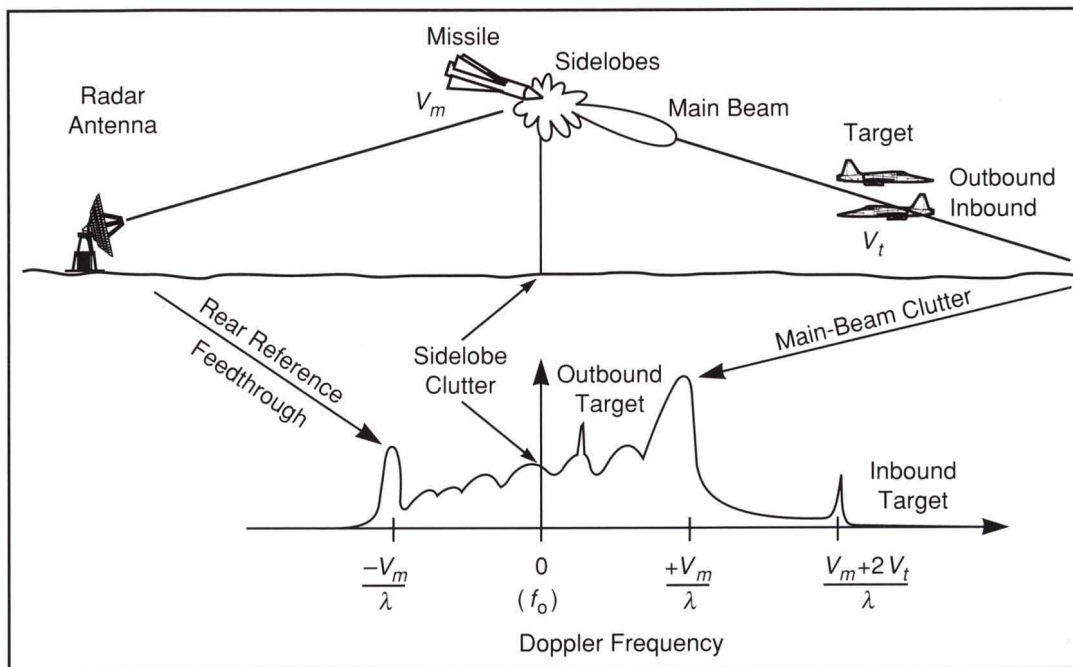


Fig. 1—Received clutter spectrum for a semi-active missile. The clutter return spreads out in Doppler frequency; clutter approached by the missile has a positive Doppler, clutter directly beneath the missile has zero Doppler, and clutter behind the missile has a negative Doppler. Incoming targets appear at a higher Doppler frequency than any clutter; outbound targets have a Doppler frequency that appears in the sidelobe clutter region.

## Radar-Guided Missiles

Radar-guided missiles exist in four basic categories: command guided, active homing, semi-active homing, and passive homing. A missile system can be designed to use each of these methods in combination. For example, a system can have command guidance for most of the missile fly-out, followed by semi-active homing in the terminal phase of flight.

A *command-guided* missile has neither a radar transmitter nor a radar receiver on board. A separate radar (usually ground based) tracks both the target and the outgoing missile and computes the trajectory changes needed to guide the missile to its target. These flight commands are communicated to the missile by a data link. The accuracy of the missile intercept is limited by the precision with which the radar can determine the target and missile locations. This precision degrades as the range to the intercept increases, leading to larger miss distances. Command guidance may be necessary when other modes of missile guidance are inadequate because of clutter, jamming, or missile receiver sensitivity problems. Many foreign missiles employ command-guidance modes because a command-guided missile does not require a complex on-board seeker system.

Missile homing guidance is needed to achieve a smaller miss distance, which is especially important for air-to-air missiles that carry small warheads. An *active* missile carries its own radar, complete with transmitter and receiver (e.g., the U.S. AMRAAM). Because of a small payload capacity and antenna

aperture, the radar on a missile is not as powerful as a ground-based or aircraft-mounted radar. To achieve long ranges on low cross-section targets, active homing must be combined with other means such as command guidance to get the missile within homing range to the target. Active missiles have the attractive features of *fire-and-forget*, which can increase the fire power of a given fire control system. A disadvantage of active missile seekers is higher cost, since a radar transmitter is required in the missile.

A high proportion of the world's radar missile inventories use a *semi-active* architecture, a scheme in which the missile carries only a radar receiver, not a transmitter (see Fig. A). The radar transmitter that illuminates the target is in a separate unit that is either ground based or airborne. This architecture has several advantages. Delivering sufficient radar energy to a target at long ranges requires high transmitter power and high-gain antennas (thus requiring a large antenna aperture), both of which are difficult to achieve on a missile constrained in weight and volume. Stronger illumination is more easily provided by a ground-based system or, to a lesser extent, by a fighter aircraft. This advantage is especially important when the target has a low radar return, which requires higher illuminator powers to achieve target detection.

Another advantage of the semi-active approach illustrated in Fig. A is that for surface-to-air missiles, which use a ground-based illuminator, the geometry

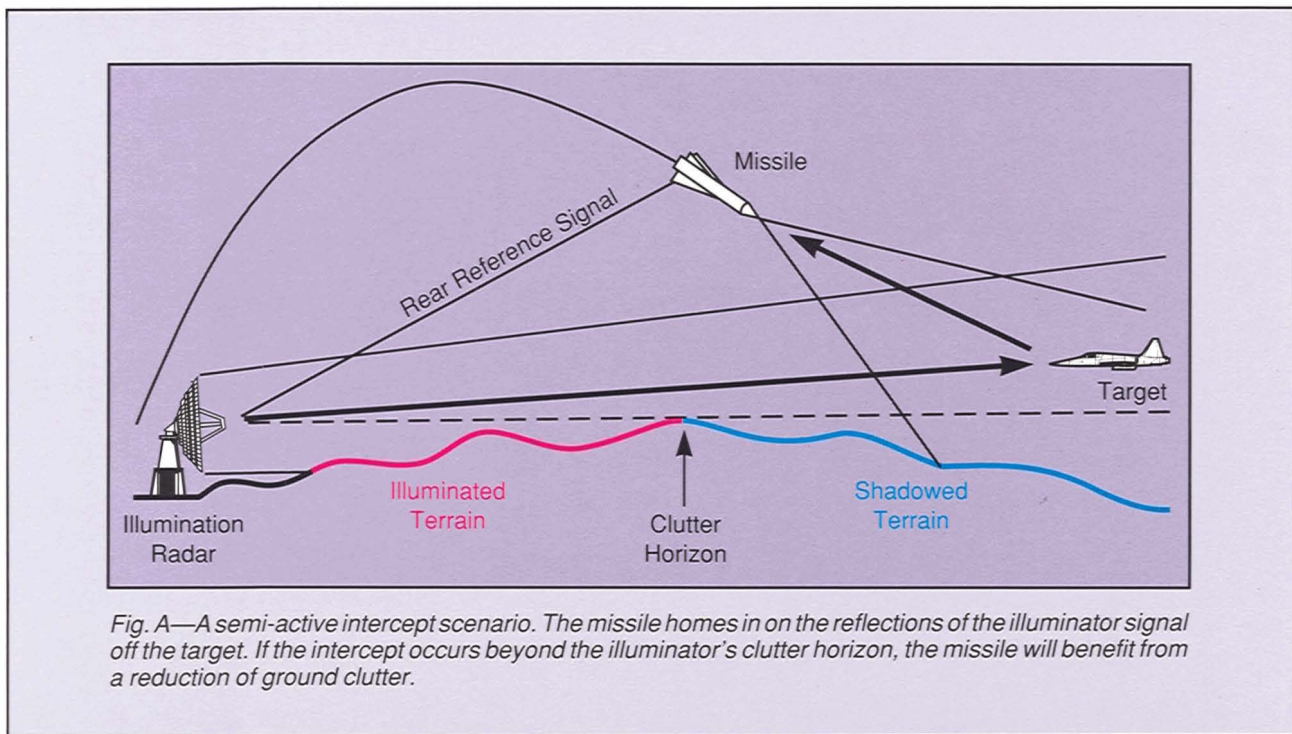
of the missile intercept can be arranged to minimize the effects of clutter. The missile antenna may be looking down at the earth, but the earth is shielded from the illuminator by intervening terrain. A further advantage of the semi-active architecture is that electronic countermeasures intended to frustrate the missile are often directed back toward the radar source. The missile is not radiating, so the target will not know the missile's location and may not be able to jam the missile seeker.

Figure A also indicates the existence of a rear reference signal. For a semi-active seeker to support coherent signal processing (such as Doppler filtering) the missile must either carry a stable frequency reference or have a receiver dedicated to listening to the direct signal from the illuminator (the rear receiver).

A *passive* homing seeker guides itself by radio emissions from the target. These emissions are from the target's own radar or other on-board radiating sensors. The advantages of passive homing are that it does not require a separate illumination radar and it operates quietly (a powerful illumination signal recognized by the target is a warning of the imminent arrival of a missile). A disadvantage is that the passive seeker depends on the presence of target emissions during homing, and these emissions are not controlled by the missile system. Another disadvantage is that the seeker must operate with a variety of different waveforms that are specific to particular targets, and these waveforms are not optimal for missile homing.

towed decoys, other fundamental techniques include wavefront distortion (known as cross-eye), for corrupting the seeker's measurement

of target angle, and terrain bounce jamming, in which a brightly illuminated spot on the ground is created to draw the



missile away from its target.

These fundamental, or *robust*, countermeasures are not as implementation-specific as the idiosyncratic type of ECM described above. Because of their fundamental nature, robust countermeasures can be investigated generically; that is, experiments can be performed that do not require specific military ECM hardware. A principal challenge for future seeker designers is to devise schemes for dealing with these fundamental types of ECM.

### Waveform Selection

Most semi-active missiles operate with CW or interrupted-CW illumination. These waveforms allow the use of Doppler filtering to separate target and clutter. The CW waveforms provide the seeker with no range information on the target; the Doppler frequency uniquely determines the relative velocity of the target.

A pulsed waveform coupled with a range-gated receiver is used to introduce additional separation of target and clutter in the range dimension. Figure 2 illustrates the reduction in clutter that can be achieved by range gating, a

technique that diminishes both the mainlobe clutter and sidelobe clutter. The pulsed waveform design is ultimately a compromise between target Doppler frequency ambiguities and target range ambiguities. The measured Doppler frequency and range values are offset from their absolute values by integer multiples of an ambiguity interval. The size of the ambiguity interval is determined by the pulse-repetition frequency. The larger the unambiguous range interval, the smaller the unambiguous Doppler interval, and vice versa. The use of multiple pulse-repetition frequencies is required to resolve these ambiguities.

A pulsed waveform is more difficult for a semi-active missile to process because the receiver must synchronize itself with the range-gate timing. The U.S. Patriot missile exemplifies one method for achieving this synchronization by sending the received signal back to the illuminator at the ground (the source of the timing) for target processing, rather than performing the necessary processing on board. Despite this complexity, however, future seekers will probably incorporate pulsed waveforms and range-

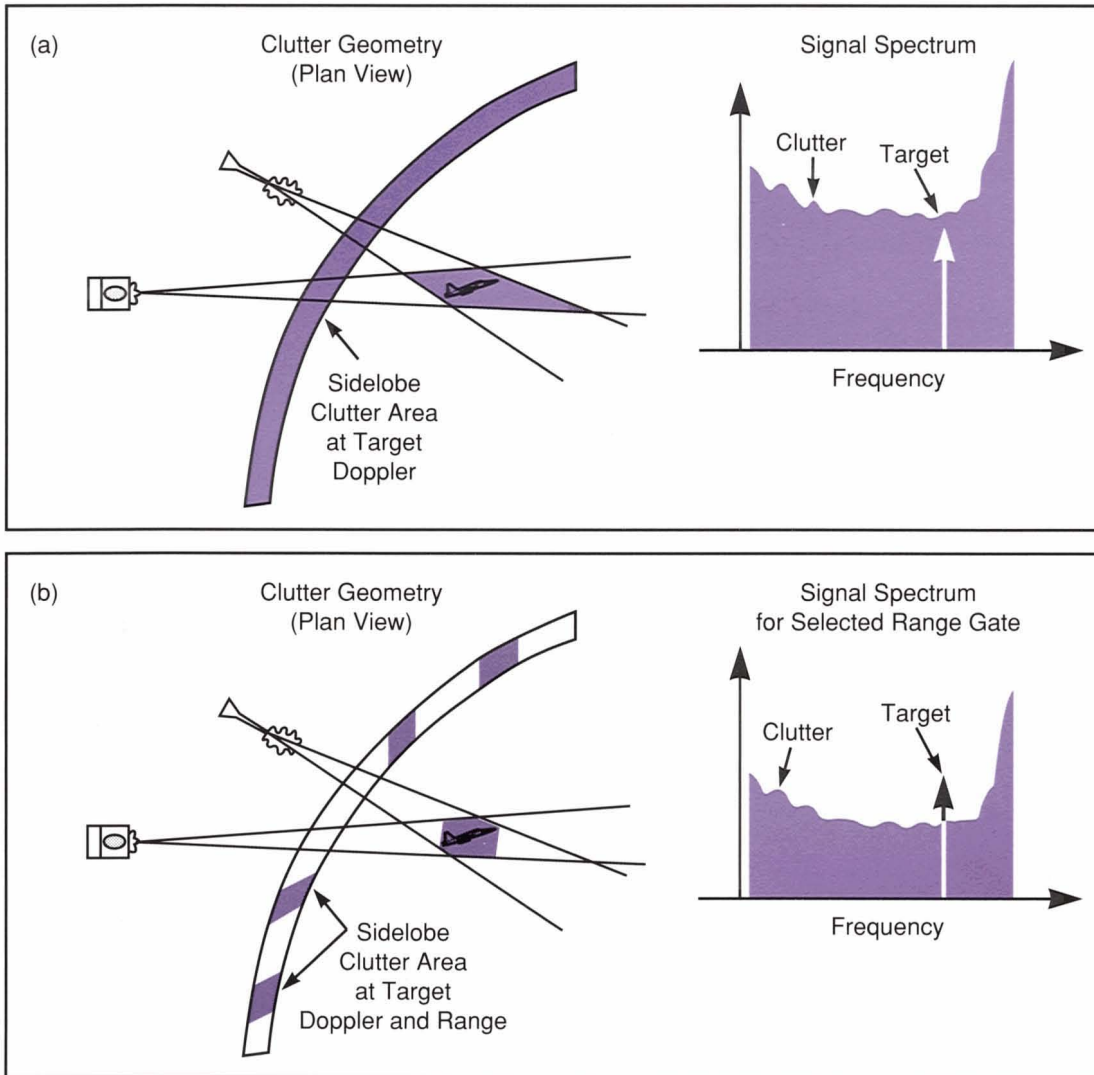


Fig. 2—A comparison of the clutter resolution of continuous-wave (CW) and pulsed waveforms. (a) For the CW waveform, different Doppler bins in the clutter spectrum divide the terrain into strips of constant Doppler frequency (called isodops). The area of ground in one of these strips multiplied by the antenna gains and clutter reflectivity value determines the strength of the clutter signal in that Doppler bin. (b) In a pulsed-Doppler waveform, consecutive signal samples represent clutter returns for different ranges from the seeker. When coupled with the resolution provided by Doppler binning, the clutter level in a given range-Doppler cell is generally reduced in comparison to CW methods because the ground area in a cell is less.

gated receivers to reduce clutter problems.

### Airborne Seeker Test Bed

Figure 3 shows the Lincoln Laboratory Airborne Seeker Test Bed that was designed to support investigations into the problems described in the previous section. Direct applications of the test bed are in the following areas:

1. Target radar cross-section measurement.

The test bed instrumentation was designed with enough sensitivity for the study of low cross-section targets. It provides dynamic in-flight dual-polarized measurements of the target radar cross section, scintillation (amplitude fluctuations), and glint (an interference effect that induces large angle-measurement errors), all measured at transmitter and receiver angles representative of missile intercept geometries.

2. *Bistatic clutter database measurement.* A dual-polarized database of bistatic (different angles to the transmitter and receiver) ground clutter can be developed for sites of interest and used in clutter modeling. Clutter measurements also support live-firing tests by helping to select the firing geometries.
3. *Measurement of operational scenarios of targets in clutter.* Target and test bed flight paths are chosen to simulate realistic intercept trajectories for evaluating target detectability and trackability.
4. *ECM evaluation.* The test bed has a high-fidelity capability to measure the signals

- generated by selected ECM. These measurements directly characterize the ECM signals, and the measured data can also be used as input to seeker system simulations that predict the ECM effect on the modeled missile system.
5. *ECCM algorithm development.* Another use for the ECM signal data is to look for discriminants, or signal features that can be used to separate false signals from the true target. New ECCM algorithms will be developed and tested on the measured ECM data. These algorithms can then be tested in real time on the test bed during a simulated intercept.



Fig. 3—Principal elements of the Airborne Seeker Test Bed on the Falcon 20 aircraft. The principal sensor, a large X-band dual-polarized monopulse antenna, is supported by a large number of instrumentation channels and a high-speed recorder. A Forward Looking Infrared Sensor (FLIR) provides an angle reference on target position for use with the radar data. A wing-mounted C-band radar locates the target and directs the other sensors.

The data obtained through the five activities listed above will be applied to the development of computer models of seeker performance, from phenomenology models (clutter, target radar cross-section dynamics) to missile fly-out models with six degrees of freedom. From these models we will extrapolate measured results to terrains other than military test ranges and evaluate the performance of new concepts for future missile systems.

The test bed represents a *captive-carry* concept (the box titled “Methods for Evaluating Missile Performance” reviews missile performance categories). A principal advantage of a captive-carry experiment is that it allows operation in the actual real-world environment and offers the possibility of repeatable trajectories and systematic profiling. A specific advantage of the Airborne Seeker Test Bed is that using a dedicated passenger jet (instead of pod-mounting the sensor equipment on a military jet) offers room for high-fidelity instrumentation and recording with operator interaction.

Whenever possible, the elements of the test bed instrumentation were designed for better performance than the corresponding elements of an actual missile. This level of performance is possible because of the advantages offered by the test bed platform. The nose-mounted primary antenna allows the use of a hemispherical radome that minimizes polarization and angle measurement distortion, and facilitates a large antenna aperture to provide increased sensitivity. The benign vibration environment provided by the jet platform supports better reference oscillator stability to improve the clutter rejection performance. Signal integration can occur over longer time periods, which further increases the sensitivity and clutter rejection of the system.

The slower speed of the test bed leads to a compressed clutter spectrum because the Doppler spread of ground clutter is proportional to the aircraft velocity. The velocity of the Falcon 20 is 2.5 times slower than the velocity of a typical missile. For the number of Doppler cells across the clutter to be comparable to a missile, the Doppler resolution in the test bed must be 2.5 times finer than in the missile. This resolution is

achieved on the test bed by extending the integration time; in fact, Doppler resolutions more than five times finer than those of a missile are practical. Note that the target spectrum is not affected by test bed speed, and the limits on target integration time due to target acceleration apply without scaling.

These important improvements in performance have been implemented so that the measured data will be more precise than the data available to a practical missile system. To model existing systems the test bed data will be degraded to match the performance of the system being studied. The original unspoiled data are important both to the phenomenology studies (clutter and target signature) and to illustrate achievable seeker performance.

### *Overview of Test Bed Hardware*

Figure 3 shows the major elements of the Airborne Seeker Test Bed. The principal payload of the Airborne Seeker Test Bed is the Instrumentation Head (IH), which is an X-band semi-active radar receiver configured as a missile seeker. The principal sensor of the IH is a large dual-polarized antenna mounted on a modified HAWK seeker gimbal. Behind the antenna are a large number of instrumented channels. Raytheon Missile Systems Division in Tewksbury, Mass., served as subcontractor on the IH and the Forward Looking Infrared System (FLIR) discussed later in the paper.

The IH receiver was designed to accommodate a variety of different waveform types, ranging from CW waveforms to experimental range-gated (pulsed) waveforms. This capability makes the IH compatible with existing illuminators such as the HAWK High Power Illuminator (HPI), the AWG-9 (on the F-14 fighter), and the APG-63 and APG-70 (on the F-15 fighter), as well as experimental and simulator radars. The Georgia Tech Research Institute (GTRI) constructed an experimental radar called the Waveform Simulator for use with the test bed, and it can generate every waveform usable by the IH. A separate radio data link from the illuminator synchronizes the IH receiver when the test bed is used with

## Methods for Evaluating Missile Performance

### Live Firing

An actual missile intercept of a target is performed in a live firing, a type of test that realistically evaluates a missile by recording true missile dynamics. A typical missile research and development program can involve 100 missile firings. The tests are limited, however, because only a few locations are available for live firings, and the amount of data collected can be limited by telemetry constraints. Also, for obvious safety reasons, live firings are not performed against manned targets, which prevents this type of evaluation of missile susceptibility for new aircraft. Live firing is also prohibitively expensive to do on more than a few geometries. Because of the limitations and expense, computer modeling is important in the design of test scenarios to ensure that the live firings yield the most useful data.

### Captive Carry

Captive-carry experiments carry a missile under the wing or

belly of a piloted aircraft. Close approximations to real intercepts can be flown, and increased instrumentation over a live firing is potentially available. Captive-carry flights can also operate against manned targets. This approach offers the possibility of more exhaustive testing in more varied environments, compared to live firing, and it is especially useful in the development of large databases (e.g., ground clutter). Captive-carry also permits the evaluation of ECM and ECCM techniques in situ.

### Hardware-in-the-Loop Simulations

This evaluation method uses a bench setup to inject signals into selected hardware components of a missile. Software simulation sequences the signals and hardware through a missile-intercept time line. This approach can be as elaborate as placing a complete seeker with antenna in an anechoic chamber, where radiating

horn antennas in the chamber represent clutter and target. Actual measured signals (from a captive carry or live firing) can be used, but the interaction of the seeker and the environment is necessarily limited. This type of test relies on the accuracy of the assumptions made in the software model. This approach is useful in exercising and evaluating specific functions of the seeker hardware and software.

### Computer Simulation

Computer simulation is the most flexible analysis technique because it can be extrapolated to cases that have not or can not be tested. It is also likely to provide the least fidelity of the listed methods because the results depend on the accuracy of assumptions used in the software model. The validity of a computer simulation is enhanced greatly by infusions of the data and experience gained from the captive-carry and live-firing tests.

experimental *interrupted illuminators* that periodically send brief bursts of illumination energy.

In addition to the IH, the test bed carries a C-band Beacon Tracking Radar (BTR) under the wing. The BTR tracks a transponder on the target aircraft and provides target-angle, range, and range-rate information in real time to the other sensors on the test bed, so that those other sensors can be tuned to the target signal even if they haven't yet detected the target. Another test bed sensor mounted under the nose is an 8-to-12- $\mu\text{m}$ -band infrared imaging device (the FLIR) that provides precision angle data on the target. A second pod un-

der the nose is currently empty and available for another optical sensor.

### Forward Sensor Antenna

The forward sensor antenna, which is the principal sensor of the IH, is a large (16-in diameter) X-band dual-polarized monopulse antenna. Figure 4 shows how the antenna was constructed as a sandwich, with an off-the-shelf slotted waveguide array that senses the vertical polarization. An array of microstrip dipoles with a microstrip feed layer embedded beneath it senses the horizontal polarization. Figure 5 is a photograph of the forward sensor

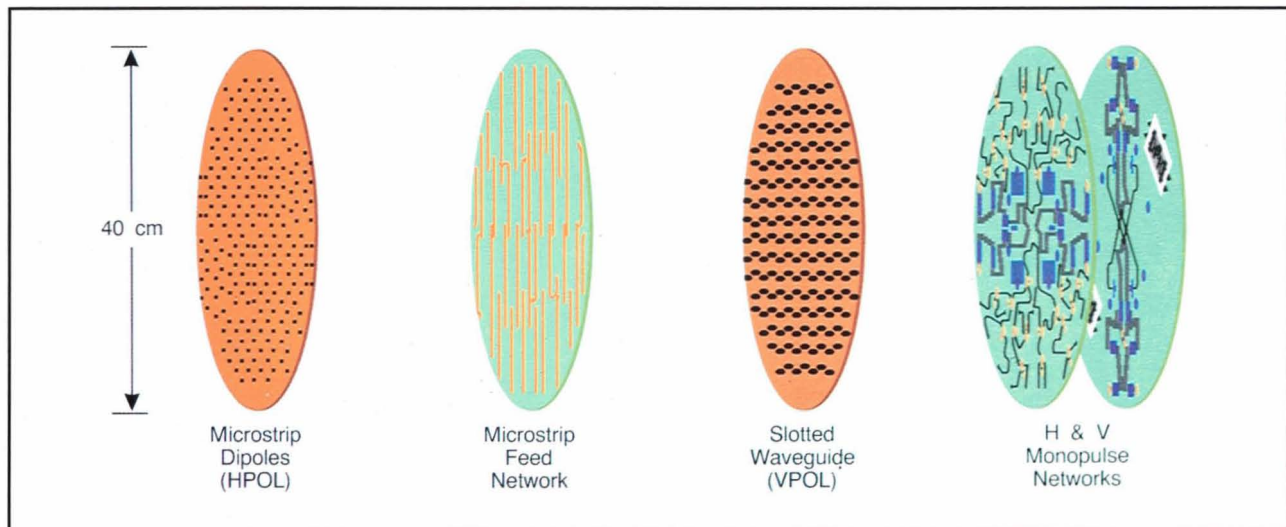


Fig. 4—The construction of the Instrumentation Head (IH) antenna. A standard slotted waveguide array (for vertical polarization) has a microstrip feed network and an array of microstrip dipoles (for horizontal polarization) layered on top of it. Two monopulse combiners, one for each polarization, are fastened to the back side of the antenna.

antenna mounted on the nose of the Falcon 20.

The signals from the vertically and horizontally polarized antenna elements are calibrated in gain and phase and combined to determine the unique polarization state of the incoming signal. The ability to make polarimetric measurements of target, clutter, and ECM signals is a key feature of the IH.

Most modern missile seekers employ monopulse tracking in which the measurement of target angle is made by comparing signal levels received simultaneously by differently shaped antenna beams. The forward sensor antenna is composed of four separate quadrants that are combined to form the signals for four monopulse components. These monopulse components are

1. *Sum beam.* This beam pattern is the normal pencil beam associated with a high-gain antenna. It results from adding the signals from all four quadrants of the antenna.
2. *Azimuth difference beam.* This beam pattern yields a null signal when the target is centered left to right. It results from subtracting signals from the left and right halves of the antenna.
3. *Elevation difference beam.* This beam pattern yields a null signal when the target is centered top to bottom. It results from

subtracting signals from the upper and lower halves of the antenna.

4. *Diagonal difference beam.* This component is not used in normal monopulse tracking, but it rounds out the complete set of linear combinations of the four antenna quadrants.

The complete set of four signals yields all of the information available from the antenna (the set of four signals represents four equations in four unknowns). In addition to monopulse processing, signal processing schemes related to ECCM can be explored by using the full set of calibrated monopulse signals. The four monopulse components in each of two polarizations (vertical and horizontal) result in eight signal channels simultaneously available to the receiver.

### Instrumentation Head Receiver

Figure 6 shows a block diagram that illustrates some of the high-level features of the IH receiver, and Table 1 summarizes the specifications of the IH receiver. The top half of Fig. 6 illustrates one of the eight forward sensor antenna channels. This channel splits into two paths: one with a wideband filter that captures the entire clutter Doppler spectrum, and one with a narrowband filter center-

ed on the target. The narrowband filter rejects the clutter signals to improve the fidelity of the recorded target signature. With a pulsed waveform, three independently controllable range gates are in each of the narrowband channels, and a split gate channel (in the monopulse sum channels only) provides a range tracking-error signal. The IH has a total of 26 narrowband channels.

The bottom half of Fig. 6 illustrates the rear receiver that receives the direct path signal from the illuminator via the rear antenna in the tail of the aircraft. The signal passes through frequency-locked and phase-locked loops to provide the stable frequency reference to mix down the front channels. The oscillator used for this function is from the AIM-7 Sparrow missile, and the rear loop design is similar to the Sparrow narrowband rear receiver.

If problems related to missiles that carry their own on-board frequency reference need investigation, the rear loop can be bypassed and a separate fixed local oscillator can be

used. In either configuration the vertical and horizontal polarization signals are recorded in the rear receiver. These two rear channels, along with the eight forward channels, make a total of 10 wideband channels in the IH.

### The Forward Looking Infrared Sensor

The role of the FLIR in the test bed is to provide a precision angle reference to the target to compare with the radar data from the IH (Fig. 7). In particular, the pointing direction of the RF seeker can be superimposed on the target image to indicate the effects of ECM. The FLIR forms a TV-compatible image from light in the infrared band (thermal radiation) with wavelengths of 8 to 12  $\mu\text{m}$ . The particular infrared device we use was manufactured by Kollmorgen and was intended for security surveillance (for example, in prison perimeter security). It was selected as a low-cost infrared sensor for angle measurement on the test bed. Because it was not designed as

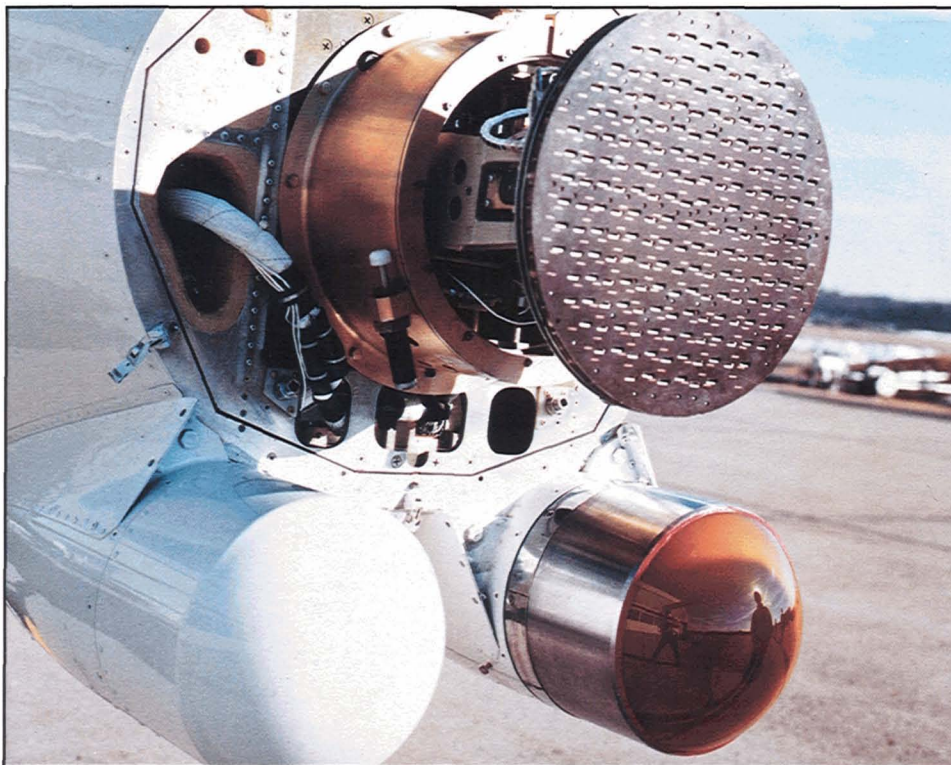


Fig. 5—The Falcon 20 nose unit is shown with the radome removed, which reveals the dual-polarized X-band antenna. The right pod holds the FLIR sensor (behind the orange zinc sulfide window). The left pod is currently empty and available for a future payload.

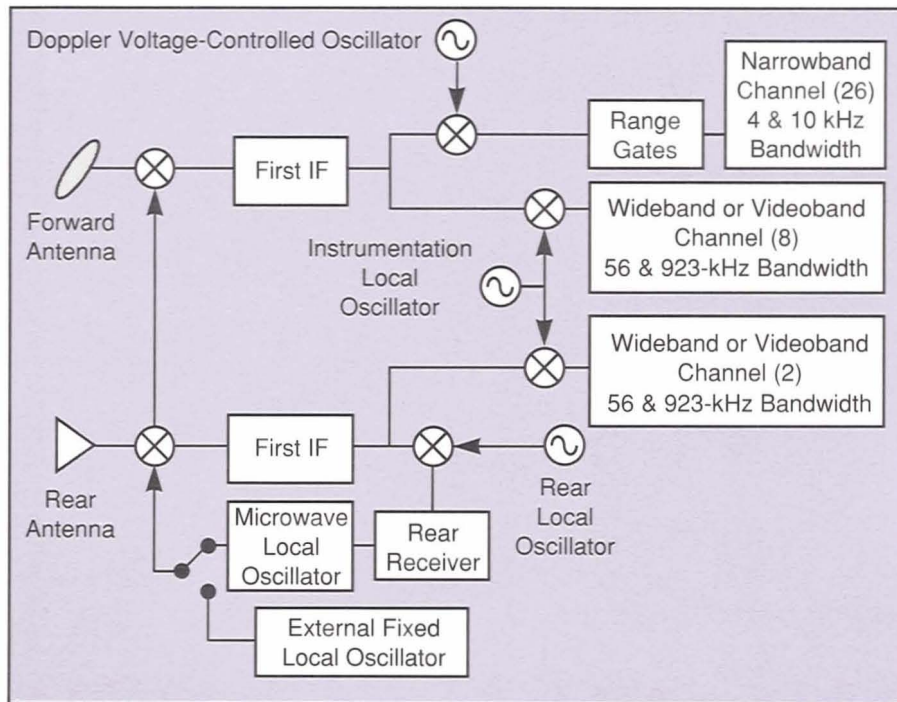


Fig. 6—A diagram of the IH receiver. The upper half of the diagram shows one of the eight forward sensor channels. The incoming signal is split into a wideband (clutter) channel and a set of narrowband (target) channels. The lower half of the diagram shows the rear receiver that locks onto the illumination signal to provide the frequency reference for tuning the front receivers.

an instrumentation system, no precise calibration of the infrared signal intensity is provided by the FLIR. Under appropriate conditions this FLIR is capable of detecting small aircraft targets at ranges on the order of 30 km.

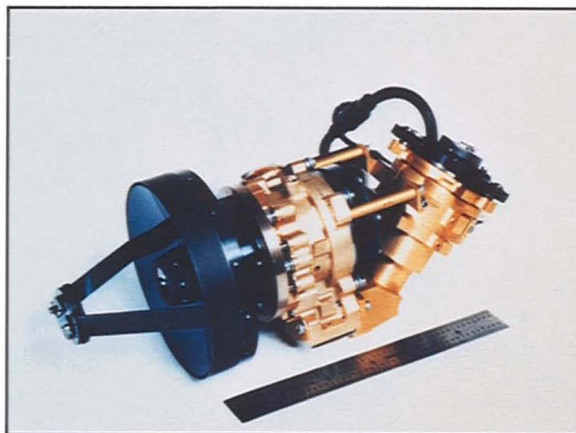


Fig. 7—The Forward Looking Infrared Sensor. The telescope mirror is visible at the front of the sensor; the structure behind it is the scanner that generates a TV format raster. The FLIR field of view is 4.5° by 3.5°. The sensor as mounted has an angular accuracy of 1 mrad (0.06°).

Mounting the FLIR in a gyro-stabilized gimbal in the nose of the aircraft provides excellent image stability; the gimbal allows the FLIR to point in the same direction as the radar antenna. A hot-spot tracker has been added to the FLIR to keep the gimbal pointed at the target. The FLIR usually will not acquire the target until the latter portion of the intercept, a limitation that is acceptable in the test bed application because the precision angle information is most important during the last phases of the intercept. Angle errors are less important to a seeker earlier in the intercept because the missile still has time at longer ranges to correct tracking errors.

### Beacon Tracking Radar

Figure 8 shows the Beacon Tracking Radar (BTR) that serves as a reference radar for the seeker test bed. The BTR, which was designed and constructed by the Sierra Nevada Corporation in Reno, Nev., is used to direct other on-

Table 1. Specifications for Instrumentation Head Receiver	
Item	Requirement
Frequency	9750-to-10,050 MHz inclusive
Signal waveforms Pulsewidth (min) PRF	Continuous wave (CW) and pulsed 0.78 $\mu$ s 20 kHz to 400 kHz
Maximum signals (at antenna port) Operating Front Rear Survivable Front Rear	-10 dBm 0 dBm  +60 dBm PK +30 dBm AVG +30 dBm PK +20 dBm AVG
Polarization of rear sensor and forward sensor	Horizontal (H) & vertical (V)
Oscillator stability Noise sidebands <15 kHz 15 kHz to 3 MHz Discrete sidebands <15 kHz  15 kHz to 3 MHz	Microwave LO dominant -80 dBc/kHz  -(80 + 20 log f/15) dBc f = frequency separation in kHz -80 dBc
System noise figure Forward sensor Rear sensor	$\leq 8$ dB $\leq 15$ dB
Receiver bandwidth Narrowband Wideband Videoband	4 kHz & 10 kHz 56 kHz 923 kHz
Coherent processing interval (CPI) For data collection For auto track	50 ms 0.5 to 16 ms
Channel-to-channel tracking accuracy (after calibration) Gain Phase	0.5 dB ( $1\sigma$ ) 3.0° rms
Absolute amplitude error (including calibration)	$< \pm 1.0$ dB
IR adjunct sensor Gimbal limits Angle accuracy (static positioning)	$\pm 50^\circ$ pitch; $\pm 40^\circ$ yaw $\leq 1.0$ mrad rms

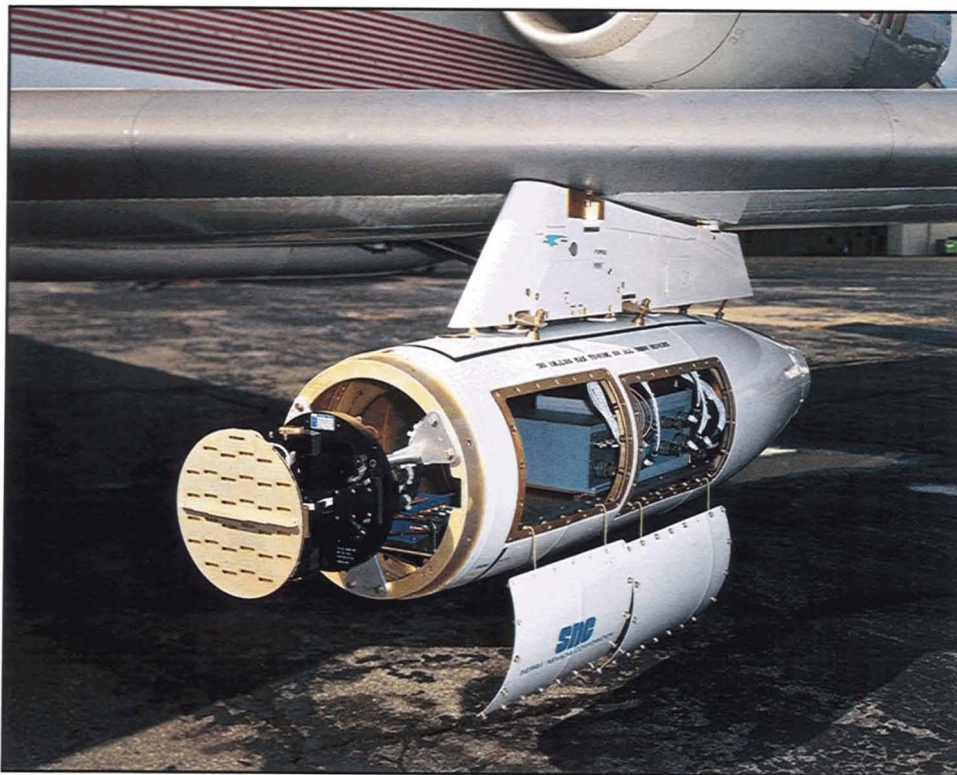


Fig. 8—The Beacon Tracking Radar (BTR). This C-band radar tracks a transponder placed on the target aircraft or at a ground reference point. The BTR records target angle, range, and range rate, which are used to aim the other test bed sensors. Valid data collection therefore begins before the other systems have acquired the target.

board sensors to the target location in angle, range, and range rate. It can locate a target prior

to acquisition by the other sensors, but only if the target has a beacon, or radio repeater, that

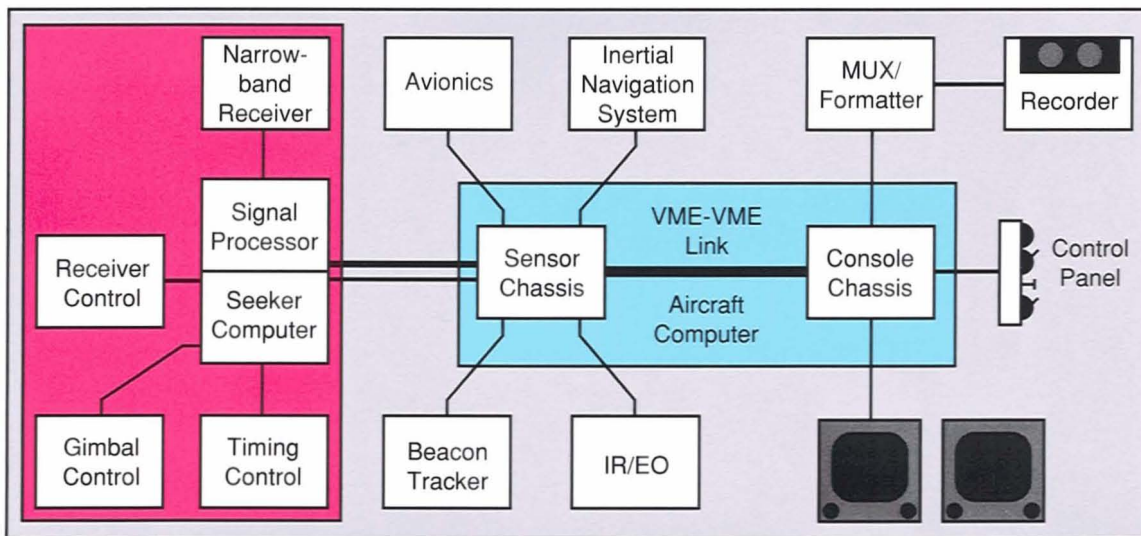


Fig. 9—A block diagram of the principal test bed computer systems. The seeker computer (shown in red) directly controls the IH (Doppler tuning, gain controls, track processing, and gimbal control). The aircraft computer (shown in blue) coordinates and records sensor reports, and represents the primary operator interface for controlling the test bed systems.

sends back a strong signal in response to the BTR interrogations. Because this signal is at a different frequency (C-band) from the other test bed sensors, signal interference does not occur. The BTR is designed to locate the target at a typical initial range of 30 km. The BTR is housed in a standard AST-4 pod and weighs 210 lbs; the other pod is empty and is used for aerodynamic balance.

## Computers and Data Recording

Figure 9 is a block diagram of the primary computers of the test bed. The red area in the figure indicates the digital system associated with the IH. This system, called the seeker computer, is responsible for receiver gain control, Doppler tuning, antenna gimbal control, and performance of the closed-loop target tracking. The blue area in the figure is the aircraft computer that controls the test bed systems. It coordinates and records the sensor reports (IH, FLIR, BTR, inertial navigation system, and global positioning system) and provides the primary operator interface for the test bed.

The computers are multitasking multi-CPU systems based on Motorola 68020 CPUs in a VME bus. Most of the system software is programmed in the C language. The signal processor is fully software programmable; the seeker and aircraft computer chassis have room to accommodate hardware enhancements and a second signal processor. These features are included to support future additions and modifications to the test bed.

The bulk of the radar data from the IH does not enter the computers; it is passed to the high-speed recorder by a custom data multiplexer developed by TEK Microsystems of Burlington, Mass. Figure 10 shows the data flow paths supported by the data multiplexer. The high-speed data recorder is an Ampex DCRSi rotary-head cassette recorder that can support data rates up to 13.3 MB/sec. Since the data rate from the IH can reach 50 MB/sec in some modes, the data multiplexer can be programmed to optimize the recording, which

allows high data rates to be supported in bursts. The data multiplexer can also support an additional DCRSi recorder.

Figure 11 is a photograph of the operator's control panel. The operator can see full signal spectra in real time and make decisions throughout the intercept. Events during a target intercept happen quickly, and not enough time is available for an operator to type commands on a computer keyboard. Consequently, specific software functions are tied to single button presses on the control panel. For example, in an ECM mission the operator might press a button to force a reacquisition in response to information shown on the screen.

After a data collection mission, a software system implemented on Sun workstations accesses and processes the data from the test bed. A single intercept flight pass can generate 700 MB of data, which can consist of 10 wide-band channels, 26 narrowband channels, and a variety of sensor reports from both on board and off board the test bed. A sophisticated architecture has been developed to allow an analyst quick and convenient access to a desired portion of the data. The analyst can then define processing operations on the data to generate the desired data products. A quick-look capability for checking data quality, generating signal spectra, and observing ECM effects is available in the field. Full data calibration and processing is performed back at the Laboratory. The analysis team at Lincoln Laboratory provides continuity of the knowledge base over the life of the project.

## Falcon 20

The Dassault Falcon 20 aircraft is a medium-sized business jet designed to carry nine passengers. Two major external modifications were made to the aircraft: wing hard points were added to support pods (a factory kit was available), and the nose was modified to support the new radome, the two optics pods, and the increased weight. The Falcon 20 airframe is rated for speeds up to 0.88 Mach, but the combination of engine performance and the increased

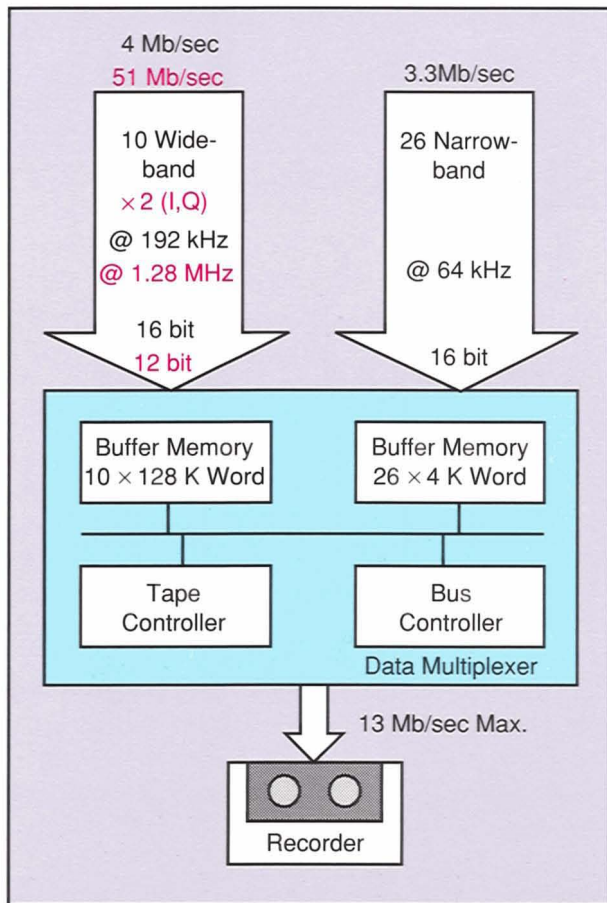


Fig. 10—A block diagram of the data multiplexer. The multiplexer is the interface between data generated by the IH and the Ampex tape recorder. Operating modes exist for continuous recording or periodic snapshots of selected channels.

drag of the external modifications limits speed to 0.73 Mach during level flight.

Figure 12 illustrates the layout of equipment in the Falcon 20 aircraft. The inertial navigation system, which is mounted in the nose on a rigid plate, produces aircraft roll, pitch, and heading readings that provide a reference for the IH antenna mount. An auxiliary power unit in the tail provides a dedicated 15 kVA of electrical power to the project. A freon cooling system installed in the tail of the aircraft handles the increased heat load generated by the project equipment.

Three test bed operators fly in the cabin along with the two pilots. One operator controls the overall system through the computer console, the second operator controls the FLIR system, and the third operator monitors signal

recording and coordinates with the ground crew.

## Test Intercept Mission

This section describes data from a typical target intercept experiment. At the time of this writing we are doing our initial testing and calibration, and have not yet collected data on any military aircraft. Although the experiment described here was designed to verify system performance, it illustrates many of the capabilities of the Airborne Seeker Test Bed.

In the test-range environment, two racetrack trajectories are set up—one for the target and one for the test bed—to provide the desired track crossing angle. (See Figure 13.) Ground controllers assist in getting the aircraft into suitable initial positions. As the test bed enters the straight leg of the intercept trajectory, the BTR acquires the target. From this point in the test, the other test bed sensors can be directed by the BTR.

The measurements described below were performed in civilian airspace over New Hampshire and Massachusetts, rather than at a test range. No ground controllers were involved (other than the local control towers that the pilots reported to periodically), and the pilots used landmarks to set up the trajectories.

The experiment was configured as a simulated head-on intercept with the test bed 170 m above the altitude of the target. The target used in the experiment was a Beechcraft Bonanza, a small single-engine propeller-driven aircraft. The test bed velocity was kept low (180 kts, or 91 m/sec) to extend data recording and to simplify pilot procedures in these initial exercises. The GTRI Waveform Simulator radar built to support the test bed provided a vertically polarized CW illumination waveform.

The signals in the following figures were received by the forward sensor antenna through the monopulse sum beams. Since the illuminator is vertically polarized, signals received through the vertical antenna channels are called *copolarized*. Signals from the horizontal antenna channels are called *cross-polarized*.



Fig. 11—The operator control panel. The upper-left screen displays received Doppler spectra; the upper-right screen lists target track-file information. The center screen displays system status and the aim point of the gimbaled sensors. The buttons on the lower panel control the stages of an intercept (data recording, sensor acquisition and reacquisition), and initiate mission-specific functions under software control.

Figure 14 shows a plot of the received Doppler spectra as a function of time. These data are taken from the wideband vertically polarized monopulse sum channel. Signal intensity is color coded as indicated; yellow represents the strongest signals. The wide bright band in the center corresponds to the ground clutter seen by the forward sensor antenna. This signal stays at a relatively constant Doppler frequency until the end of the trajectory, when the test bed flies beyond the strong clutter sources. As the test bed flies over a clutter source, its Doppler frequency decreases. The narrow Doppler line to the right of the clutter is the incoming Bonanza aircraft. The characteristic

drop in its Doppler frequency as the test bed flies past is clearly evident in the figure at approximately 50 sec.

Figure 15 shows a single Doppler spectrum taken from the narrowband copolarized (vertical) monopulse sum channel at 33 sec into the run. The received signal is integrated for 64 msec, which when processed with a Kaiser-Bessel windowing function yields a Doppler resolution of 40 Hz. The Doppler frequency of the central target line is slightly over 10 kHz, which corresponds to a closing velocity of 315 kts (160 m/sec) between test bed and target. We can see certain characteristics of the Bonanza target surrounding the central Doppler line (the *skin*

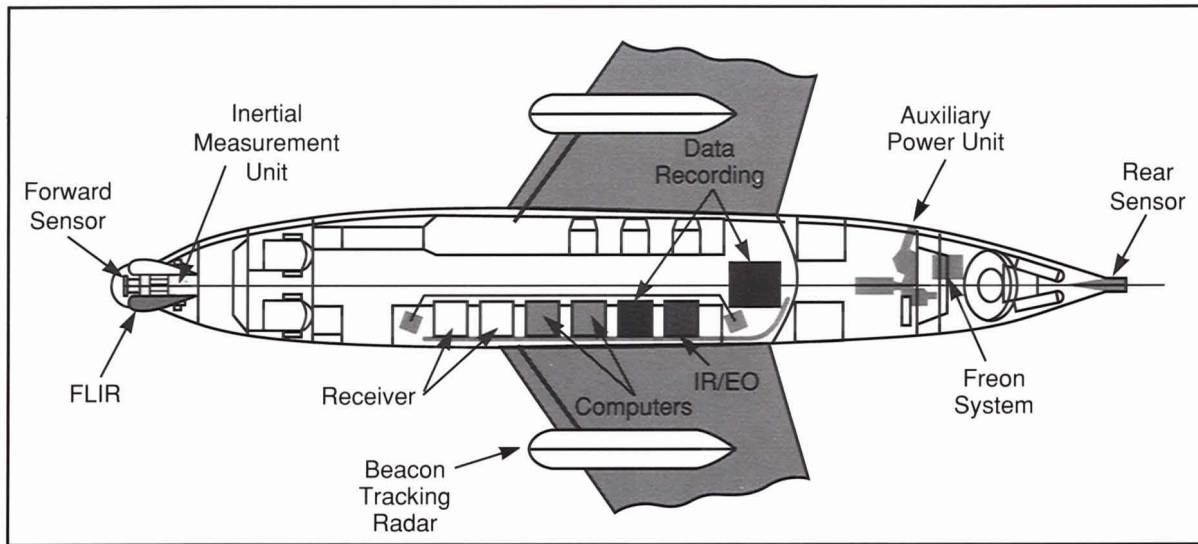


Fig. 12—Layout of equipment in the Falcon 20. The inertial measurement unit in the nose determines the roll, pitch, and heading values of the test bed as well as its position in space. Most of the system electronics are in the racks along the left side of the aircraft. The auxiliary power unit in the tail provides the electrical power for all of the project equipment.

return). The broadened region of Doppler sidebands is due to propeller modulation of the radar signals; this broadening is also visible in the spectra of Fig. 14. Similar modulations

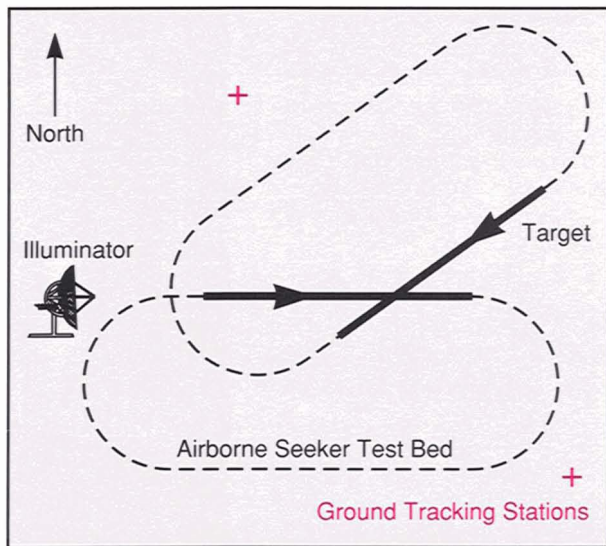


Fig. 13—The flight-path geometry for a simulated intercept. The test bed flies radially outbound from the illuminator. The racetrack path of the target is oriented to yield the desired crossing angle between test bed and target. Ground controllers direct both aircraft to cause the intercept to occur at a selected location. The test bed is 170 m higher than the target for safety reasons and for providing a look-down geometry.

appear on jet aircraft targets if the engine turbine blades are visible.

Figure 16 shows the signal strength of the Bonanza skin return during the first 50 seconds of the fly-by. The signals for the copolarized (V-pol) returns and cross-polarized (H-pol) returns were measured simultaneously during the fly-by. The copolarized signal tends to dominate, but the cross-polarized return is frequently seen to be stronger.

Figure 17, which shows the instantaneous polarization state of the target over a brief interval of time, is another representation of the radar cross-section data. The coordinates shown are a rectangular projection of the Poincaré polarization sphere, which has left-hand circular (LHC) polarization at the north pole, right-hand circular (RHC) polarization at the south pole, and a range of elliptical polarizations in between. The linear polarizations at various rotation angles are represented around the equator. If the Bonanza did not depolarize the incident vertically polarized signal, we would see the return signal clustered at V-pol, indicated by the large dot in the center of the figure. The various scattering centers on the aircraft distort the incident polarization, however, and

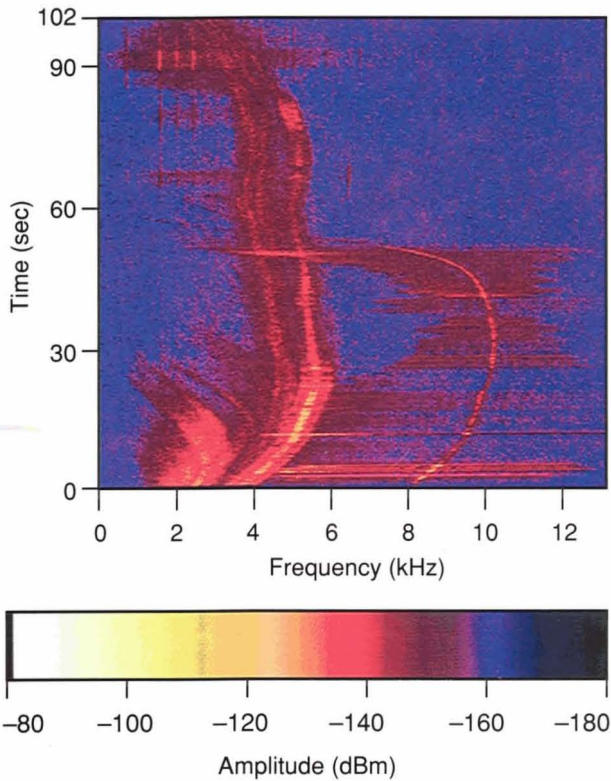


Fig. 14—The received Doppler spectra as they evolved in time during the intercept. The legend shows signal intensity encoded as color. The bright stripe at 5 kHz is ground clutter seen through the sidelobes of the IH antenna. The target signal is visible as the narrow stripe at 10 kHz. The test bed passes the target at approximately 50 sec, when the target Doppler rapidly falls off. The figure also shows a spreading of the target Doppler spectrum because of signal modulations caused by the propeller on the Bonanza aircraft.

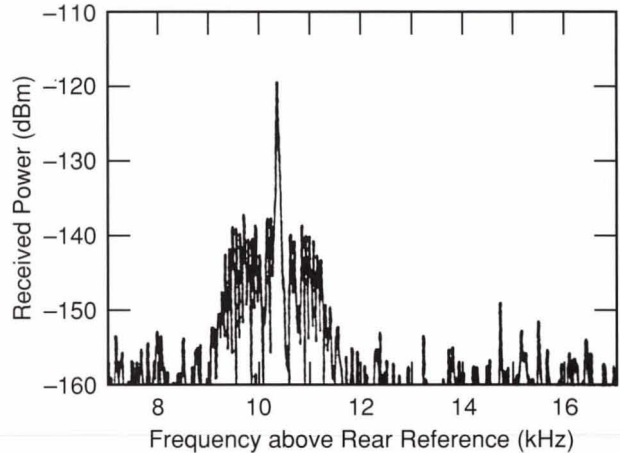


Fig. 15—Measured Doppler spectrum in the narrowband monopulse sum channel for the copolarized return signal, at a point corresponding to 33 sec in Fig. 14. The Bonanza return appears at 10 kHz. The character of the propeller modulations is clearly evident as the widely spread base region around the central skin line. The narrowband plots were processed to a Doppler resolution of 40 Hz.

these individual contributions combine with various phase shifts to yield the complicated behavior shown.

For comparison, Fig. 18 shows the corresponding polarization return with the antenna main beam centered on clutter (this measurement was made separately from the Bonanza intercept). Note that the clutter depolarizes the V-pol illumination signal significantly, but the data are distributed and clustered differently

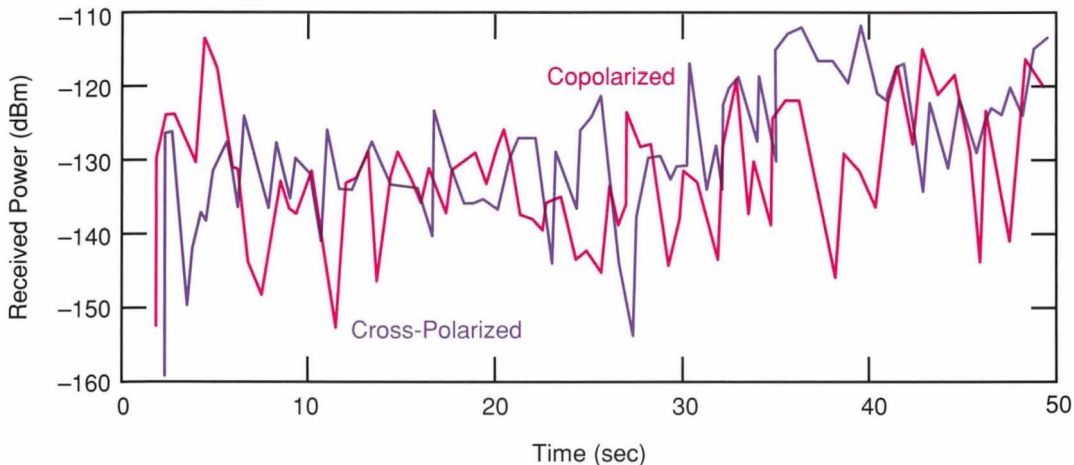


Fig. 16—A plot of the signal strength (in dB below a milliwatt) of the target skin return versus time for both the copolarized and cross-polarized components. Even though the illuminating signal is vertically polarized, the signal scattered by the target is dominated by the vertical component only half the time.

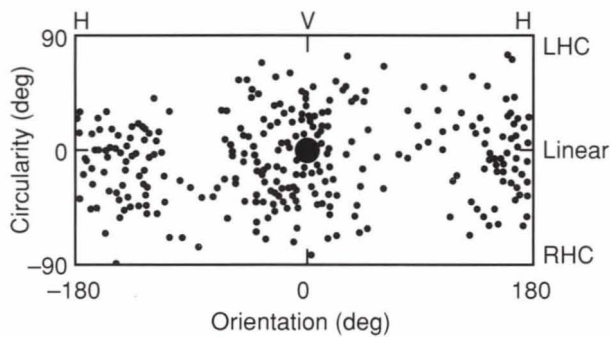


Fig. 17—The true polarization state of the target return is derived from the amplitude and phase of the received vertical and horizontal polarized signal components. The polarization state is plotted here on a rectangular representation of the Poincaré sphere. The equator of this sphere is the locus of linear polarizations that range from horizontal on the left to vertical in the middle to horizontal on the right. Up and down excursions on the plot represent increasing ellipticity in the received polarization, with left-hand circular (LHC) polarization at the north pole (the top edge of the graph), and right-hand circular (RHC) polarization at the south pole (the bottom edge of the graph). The received polarization, though fairly random, forms two distinct clusters, one around vertical polarization and one around horizontal polarization. The center dot indicates the vertical polarization of the illumination signal.

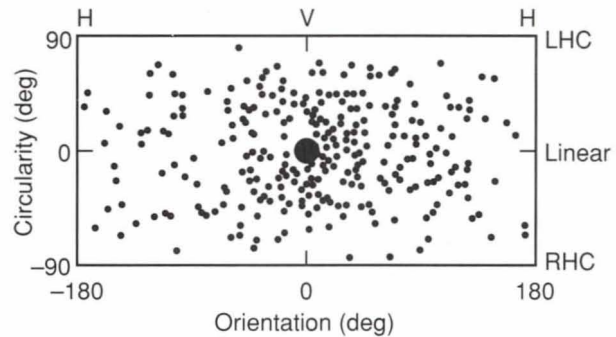


Fig. 18—The polarization state of an interval of clutter data plotted on a rectangular representation of the Poincaré sphere. Even though the received polarization is diffusely distributed, it clusters around the center dot that indicates the vertical polarization of the illumination signal.

from those of the target returns of Fig. 17.

Figure 19 shows an FLIR image of the Bonanza as it appeared at a range of 0.8 km. For most of an intercept the target aircraft is unresolved; it appears as a single pixel on the video screen. At this close range, the Bonanza outline is seen as dark (cool) against the warmer earth background. The bright spot on the nose of the aircraft is the exposed hot engine. A computer-generated cross hair superimposed on the FLIR video indicates the radar aim point obtained from the IH. The motion of the cross hair provides a visual indication of the dynamic behavior of the radar track and is useful for demonstrating the degree of ECM angle deception. In Fig. 19 the cross hair to the left of the Bonanza aircraft shows where the IH was positioned at the time, and is shown only for illustration.

## Summary

Lincoln Laboratory's Airborne Seeker Test Bed represents a powerful tool for investigating missile seeker performance. The ability to collect

high-fidelity data in a repeatable and systematic measurement program makes the test bed especially valuable for investigating advanced seeker concepts and electronic countermeasures and for developing signal processing schemes to defeat countermeasures. Though only in the air for a few weeks as of this writing, the test bed has already demonstrated the basic functionality required for its mission, from the proper performance of all sensor systems, operating modes, and data recording to the execution of clutter and target intercept measurements.

In the near future the Airborne Seeker Test Bed will operate at White Sands Missile Range in a variety of tests involving clutter, target, and ECM measurements, with ground-based and airborne illuminators. A database of bistatic desert clutter will be collected and compared to results from other clutter measurements made at the same locations. Bistatic target radar cross-section measurements will be collected on a T-38 aircraft both to demonstrate test bed capabilities and to perfect flight procedures. Both ground-based and airborne illuminators will be used in the clutter and target measurements. Intercepts will be performed on aircraft equipped with angle-deception ECM to investigate the jamming characteristics and identify possible discriminants.

After the tests at White Sands a number of tests are planned with other air vehicles of Air Force interest to investigate their specific vulnerabilities to missile seekers. Long-term plans for the test bed include the development and

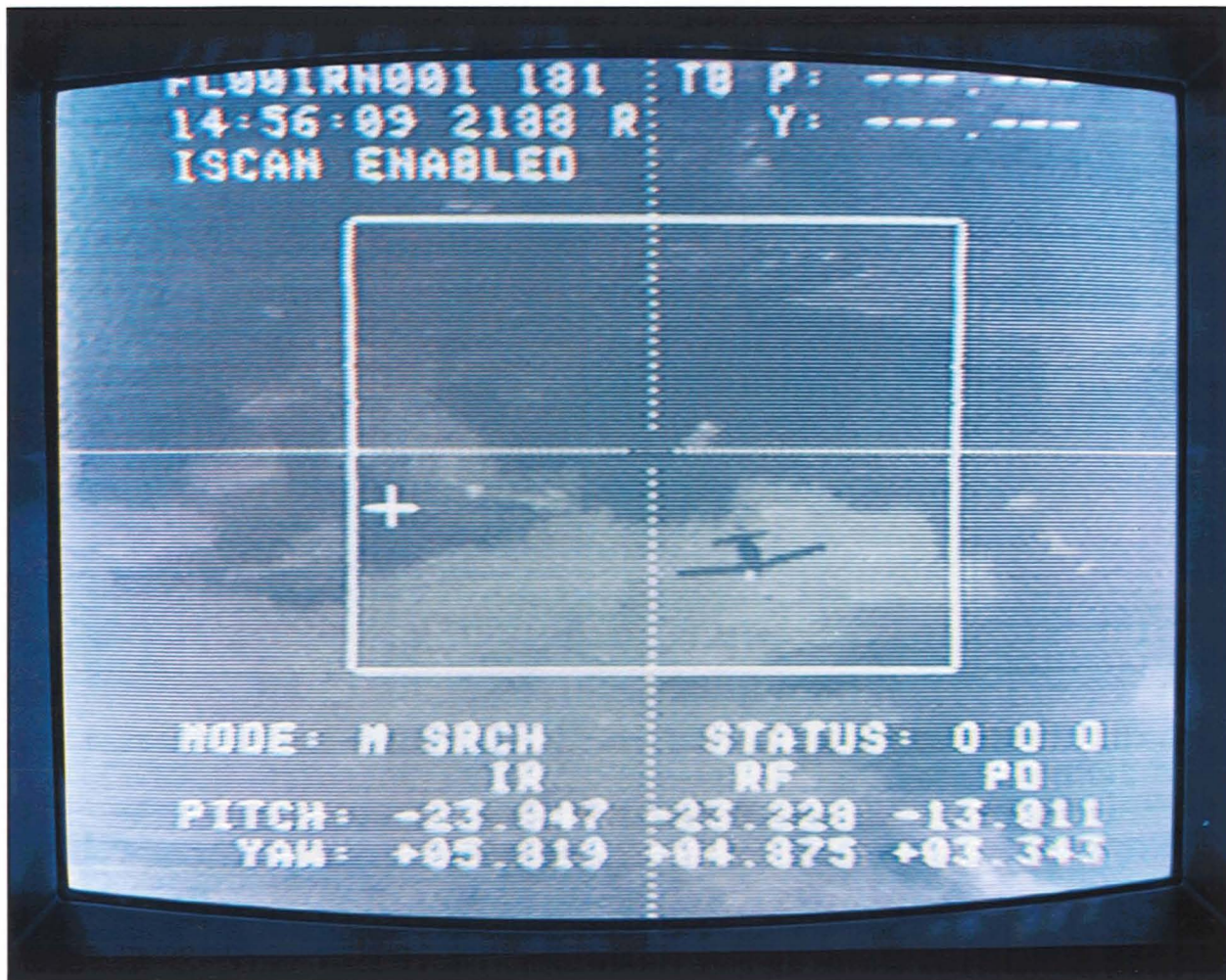


Fig. 19—A FLIR image of the target Bonanza aircraft, taken near the end of the intercept at a range of 0.8 km. The hot engine parts appear as a positive contrast (brighter) against the earth background, while the body and wings of the aircraft appear as a negative contrast (darker) against the warm earth. A computer-generated cross hair superimposed on the FLIR video indicates the aim point of the IH radar.

demonstration of advanced ECCM algorithms, the addition of other sensors, and the flying of advanced-concept brass-board seekers.

### Acknowledgments

The Airborne Seeker Test Bed was developed under the joint sponsorship of the Air Force and the Army. I would specifically like to acknowledge Dr. David L. Briggs of Lincoln Laboratory and Lt. Col. James P. Hogarty of the Air Force, the originators of the seeker test bed concept. Colonel Hogarty and Joseph Durham of the Army Missile and Space Intelligence Command provided the sponsorship necessary to make this project a reality. Program direction and

support is currently being continued into the operational phase by Lt. Col. Phil Soucy of the Air Force.

A complex project necessarily relies on the hard work and careful attention of a large group of people. Their tireless help has been and continues to be essential to the success of the project. Many people have been involved in the test bed development, including numerous Raytheon contributors. I will mention only the principal members of the Airborne Seeker Test Bed subcontractor teams: Raytheon program manager Victor Weisenbloom, Larry Durfee, and Tom Clougher, all of the Raytheon Missile Systems Division; Andy Reddig of TEK

Microsystems; and George Clary and Stan McDonald of the Sierra Nevada Corp.

The Lincoln Laboratory personnel who have seen the test bed into first flight are Group Leaders Dr. Lewis Thurman and Dennis Keane; system engineers Louis Hebert, Paul Juodawlakis, Dr. Randy Avent, and Dr. Al Hearn; software developers Ken Gregson,

Jim Clarke, Al Shaver, David Bruce, Dan Sparrell, Dave Kohr, Pete Szymansky, Cynthia Eldridge, and Lucy Smiley; engineers Dick Simard, Mark Green, and John Parkins; technical assistants Al Davis, John Allen, Bob Cavanaugh, and Dick Thibodeau; pilots Charlie Magnarelli and Mike Radoslovich; and chief mechanic Bob Murray.



CURTIS W. DAVIS III is the Assistant Leader of the Air Defense Techniques Group. He received his B.S., M.S., and Ph.D. degrees from the Ohio State University, where he worked on impulse radar for underground probing.

While at Ohio State he built ultrawideband measurement systems, designed antennas, and mathematically modeled radar performance. Since joining Lincoln Laboratory in 1979 Curt has been involved in the instrumentation and performance analyses of air defense radar systems. His activities have included adding computer recording capability to an X-band ground-clutter measurement radar; the design, construction, and operation of a helicopter-mounted field-strength measurement system for multipath profiling; development of multipath modeling algorithms; and various radar system analysis activities. Curt was responsible for defining the basic architecture and specifications of the Airborne Seeker Test Bed system, and he serves as the test bed's project engineer.